

Design and Characterization of a Neutron Calibration Facility for the Study of sub-keV Nuclear Recoils.

P.S. Barbeau^a, J.I. Collar^{a*} and P.M. Whaley^b

^aDepartment of Physics, Enrico Fermi Institute and Kavli Institute for Cosmological Physics
University of Chicago, Chicago, IL 60637, USA

^bDepartment of Mechanical and Nuclear Engineering,
Kansas State University, Manhattan, KS 66506, USA

As part of an experimental effort to demonstrate sensitivity in a large-mass detector to the ultra-low energy recoils expected from coherent neutrino-nucleus elastic scattering, we have designed and built a highly monochromatic 24 keV neutron beam at the Kansas State University Triga Mark-II reactor. The beam characteristics were chosen so as to mimic the soft recoil energies expected from reactor antineutrinos in a variety of targets, allowing to understand the response of dedicated detector technologies in this yet unexplored sub-keV recoil range. A full characterization of the beam properties (intensity, monochromaticity, contaminations, beam profile) is presented, together with first tests of the calibration setup using proton recoils in organic scintillator.

1. INTRODUCTION

The scattering of low-energy neutrinos off nuclei ($E_\nu < \text{few tens of MeV}$, e.g., reactor $\bar{\nu}_s$) via the neutral current remains undetected thirty years after its first description [1]. The small momenta exchanged at these neutrino energies result in the entire nucleus being probed, giving rise to a large coherent enhancement to the cross section, roughly proportional to neutron number squared [2]. The resulting cross section is very large compared to other low-energy neutrino interaction channels. This process is quantum-mechanically possible due to the indistinguishability of initial and final target states, having no charged-current equivalent. Using this mode of interaction, it would be possible to imagine smallish neutrino detectors: in some experimental conditions the expected rates can be as high as several hundred recoils/kg day [2,3], by no means a “rare-event” situation. However, the recoil energy transferred to the target is of a few keV at most for the lightest nuclei, with only a few percent of it going into readily measurable channels (ionization or scintillation). As a result of this, no realistic detector

technology has been available with the combination of mass and energy threshold capable of a first measurement of this intriguing mode of neutrino interaction.

This paper is part one of two: here the steps taken to demonstrate sensitivity to sub-keV recoils in a variety of detecting media by means of a low-energy highly monochromatic neutron beam are delineated. In a companion paper [4] a new detector technology (a large-mass modified electrode p-type germanium diode) finally able to exploit this mode of neutrino interaction is described, as well as the expected performance and applications of this detector in fundamental and applied neutrino physics, and in other areas (e.g., dark matter searches).

2. A CALIBRATION FACILITY FOR COHERENT NEUTRINO DETECTORS, MINUS THE NEUTRINOS

Devising a method able to accurately determine the response of a detector to sub-keV recoils is almost as difficult as developing a technology sensitive to these. The first coherent neutrino detector will be entering a low-energy *terra*

*contact author: collar@uchicago.edu

incognita, never explored before with devices of any significant mass. It would be foolish to expose a capable detector to a high-flux of reactor antineutrinos to then claim that a low-energy excess dangerously neighboring the electronic noise originates in the sought recoils: a very precise understanding of quenching factors (i.e., the fraction of the recoil energy available for detection in the form of ionization, scintillation, etc.) in this energy region is a must, prior to exposure to a neutrino source. Towards this end at least two methods have been put forward. One relies on the recoiling daughters (of up to a few hundreds of eV) that accompany high-energy gamma emission following thermal neutron absorption [5,6]. The disadvantage of this approach is a very limited choice, if any, of intense enough gamma-emitting transitions leading to energetic enough recoils in any given detector material. An aggravating factor is that not all decays produce predictable energy depositions, due to prompt secondary gamma emission while the recoil is still slowing down [6]. A better approach [3] is to rely instead on the existence of narrow deep interference “dips” in the neutron cross-sections in a handful of isotopes (Fig. 1): this can be exploited to build transmission filters in nuclear reactor facilities that allow neutrons only in those precise energy bands to percolate [7]. In the case of an iron filter, the 24 keV (± 2 keV FWHM) neutron emission is ideal to mimic the recoil energies expected from reactor antineutrinos (Fig. 2) [3]. Iron is a good gamma shielding material and well-designed filters of this type generally exhibit a very low contamination with these or with neutrons in other energy ranges [7]. An additional aluminum post-filter has the effect of reducing the overall neutron flux, but preferentially at larger than 24 keV energies, i.e., results in a higher beam purity (Fig. 1). A thin (~ 1 cm) removable titanium post-filter can be used to scatter away the 24 keV component without affecting other beam components (i.e., the backgrounds), a result of a resonance in the Ti neutron cross-section, centered precisely around this energy (Fig. 1). This provides a unique opportunity to perform “signal on” and “signal off” runs, allowing the experimenter to make sure that tiny recoil-like signals

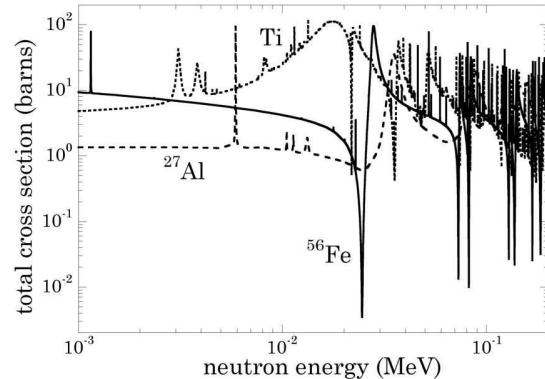


Figure 1. Neutron cross-sections of relevance in the design of a 24 keV iron filter beam. Aluminum is considered an ideal post-filter material, able to preferentially suppress surviving neutron energies >24 keV. Titanium can be used to “switch off” the main 24 keV component, while leaving all other neutron energies and any gamma rays essentially unaltered.

are indeed originating from the 24 keV component and not in any beam contamination, no matter how secondary. The beneficial effect of this on the credibility of the results cannot be overemphasized.

2.1. Design of a 24 keV neutron beam

A present penury of iron filter reactor beams in the US lead to the design and construction of a dedicated, easily-removable filter at the University of Chicago, for installation in the Kansas State University TRIGA Mark-II experimental reactor. MCNP4b [9] simulations using available spectral measurements of unfiltered tangential beam neutron emissions as the input, revealed that a narrow (2.5 cm diameter, 60 cm long) filter extremely low in non-Fe contaminants [10] would produce an equivalent beam intensity and purity to a larger diameter, lower quality iron rod, which is a more common approach [7] (“beam purity” is the fraction of the total neutron flux falling under the 24 keV peak). Fig. 3 displays an schematic of the final design. These simulations (Fig. 3, bottom) demonstrated that a high-

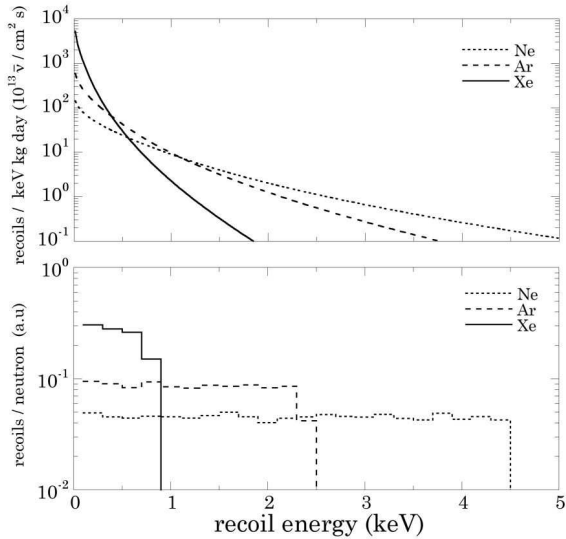


Figure 2. Top: Spectrum of recoil energies expected from reactor antineutrinos in several target materials. Bottom: Recoil spectrum similar in energy span, from exposure to a 24 keV neutron beam (MCNP-Polimi simulation [8]).

enough 24 keV flux and purity should be available even from a low-power experimental reactor (240 kW max., with a current upgrade to 1.25 MW pending). During initial testing, a gamma background ignored in the simulations was observed (50 mRem/hr on contact), streaming from the concrete in the periphery of the beam, originating in moderation and capture of neutrons once-scattered in the back of the filter. This background was controlled with the addition of 50 cm of high-density concrete and Pb shielding around the beam exit.

2.2. Beam Characterization

2.2.1. Neutron flux and angular divergence

Neutron flux measurements using a “Benjamin” spherical proton-recoil spectrometer [11] placed both along the beam axis and off-axis revealed a measurable angular divergence. An equivalent point source, derived from axial measurements, was seen to reside -36.1 ± 4.8 cm into

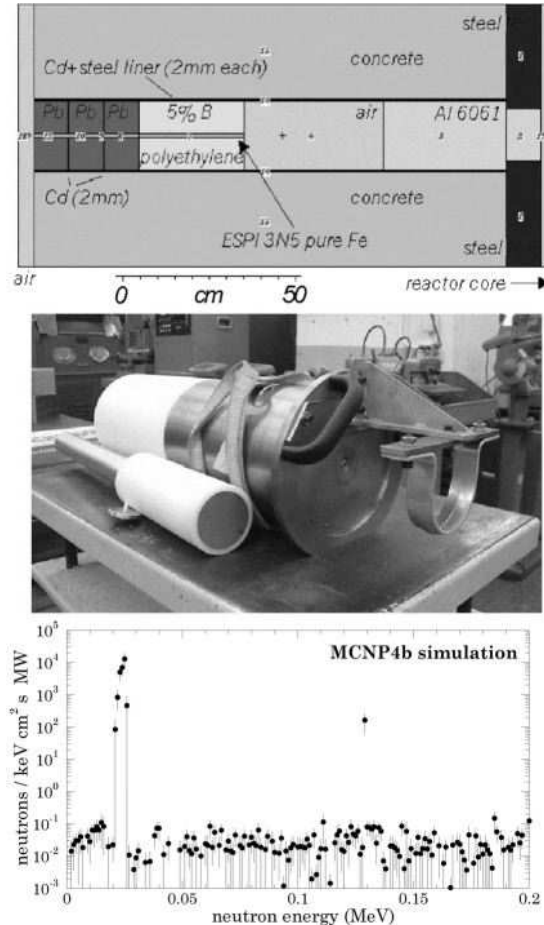


Figure 3. Top: Schematic design of the UC/KSU filter. The Fe rod was machined with a tapered cross-section to avoid streaming of radiation. The Al spectrum shifter was removed in the final configuration. Middle: Completed filter, with Al/Ti post-filter holder visible in the foreground. A laser alignment tool can be screwed onto the Fe rod, allowing precise detector placement. Bottom: Predicted beam composition.

the filter (taking the exit point as the origin of coordinates), in good agreement with a geometric neutron optics estimate ($z = -35.9$ cm). Based on off-axis measurements, the beam lateral spread at the $z = +110$ cm location (the chosen detector

calibration point) was observed to span ~ 6 cm FWHM. This was confirmed by careful mapping of this spread with a small (1 c.c.) ${}^6\text{LiI}(\text{Eu})$ scintillator [12], 95% enriched in ${}^6\text{Li}$, surrounded by 0.5 mm of Cd to reduce response to thermal neutrons. The 2-d mapping resulting from measurements over a 10×10 grid of positions, displayed in Fig. 4, is an accurate description of the local neutron flux at the detector irradiation point. The 24 keV neutron flux component was extracted from the counting rate difference between Ti-on and Ti-off operation, with a detector efficiency (reaction rate) derived from MCNP4b simulations. The maximum beam intensity at the filter exit was measured using the proton-recoil spectrometer at 7.9×10^4 ($\pm 10\%$ stat. $\pm 15\%$ sys.) $\text{n cm}^{-2} \text{s}^{-1} \text{MW}^{-1}$, a typical value for Fe filter designs [7].

2.2.2. Monochromaticity and beam contaminations

Additional measurements of axial beam intensity, composition, effect of filters and radial divergence were performed using the proton-recoil spectrometer, a ${}^3\text{He}$ ionization chamber and a HPGe gamma detector. The first allows to perform high-resolution neutron spectroscopy by deconvolution (unfolding) of its response, down to ~ 1 keV neutron energies [14]. Figs. 5-7 encapsulate these results (datapoints in Fig. 5 and top Fig. 6 are modestly smoothed to facilitate comparison and deconvolution). The beam purity obtained in the presence of a 2.5 cm Al post-filter [13] is $\sim 88\%$ (Fig. 5), as measured at $z=+110$ cm. The marked decrease in >24 keV recoils by the addition of the Al post-filter is clearly observed in the figure, at the expense of a comparatively much smaller decrease in the 24 keV component. This effect can be understood by inspection of the neutron cross-sections in Fig. 1.

Fig. 6 (top) displays the dramatic effect of the addition of a 1.25 cm-thick Ti post-filter: the 24 keV peak intensity is squelched by a factor ~ 20 , in agreement with simulations, while the comparatively smaller flux of neutrons at all other energies remains essentially unaffected, providing a way to “switch off” exclusively the source of the soft recoils of interest. The response of the proton-

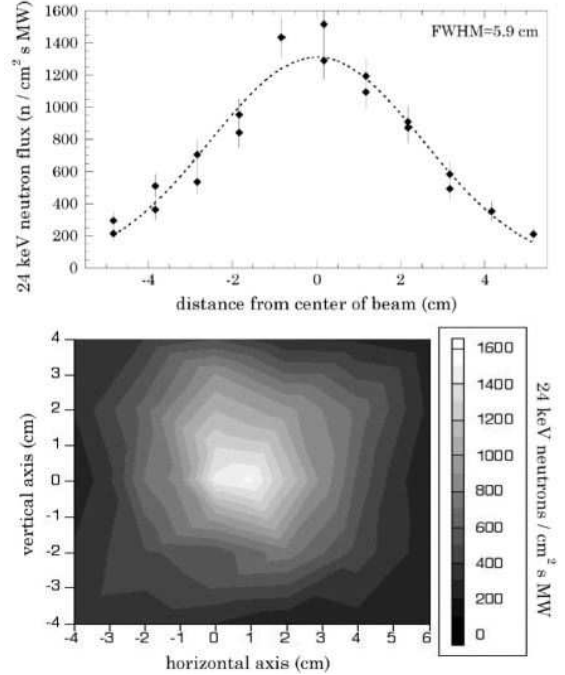


Figure 4. Top: Beam profile characterization at the detector irradiation point, 110 cm in front of the beam exit, using a small enriched ${}^6\text{LiI}(\text{Eu})$ scintillator. Bottom: A 2-d image of the same, revealing a small lateral misalignment of ~ 0.5 cm, a measure of the present ability to center detectors under test with the beam, using a laser tool.

recoil spectrometer to an intense (3 mCi) ${}^{88}\text{Y}$ high-energy gamma source is normalized in the figure to the maximum of the Ti filter spectrum, illustrating the marginal sensitivity to gammas in this type of detector, which allows to perform low-energy neutron measurements [14]. The inset is the deconvolution of the proton recoil spectrum to generate a neutron energy spectrum, using the SPEC-4 code [15]. It clearly demonstrates the good monochromaticity achieved and the extinction of exclusively the 24 keV peak in the presence of Ti. This was also confirmed by the ${}^3\text{He}$ measurements (Fig. 6, bottom), using this type of counter as a rudimentary spectrometer. The non-proportionality of this last detector results

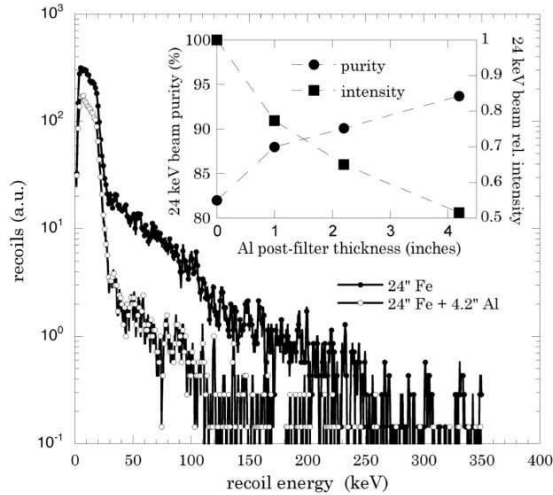


Figure 5. Effect of an Al post-filter in increasing the purity of a 24 keV Fe neutron filter (“purity” defined as the percent of neutrons emitted falling under the 24 keV peak). The spectra (same exposure) are measured using a spherical (“Benjamin”) hydrogen-filled proton-recoil spectrometer. Recoil energies of up to the incident neutron kinetic energy are possible in this type of detector.

in a much diminished energy resolution in the unfolded spectra, but identical beam components are revealed. The small higher energy components (72 keV, 128 keV, etc.) discernible in both proton-recoil and ^3He unfolded spectra are typical of Fe filters [7,17] and the result of second-order passing bands in the Fe cross-sections (Fig. 1, 3 bottom), not entirely canceled by the Al post-filter.

The effect of the thin Ti post-filter on gamma backgrounds is also negligible, leading to a mere 6% reduction in overall gamma flux (Fig. 7). The presence of several characteristically asymmetric peaks in the HPGe spectrum, arising from inelastic neutron scattering, (Fig. 7, inset) allows to impose further limits on the neutron component at energies >691 keV [18] (less than $100 \text{ n cm}^{-2} \text{ s}^{-1} \text{ MW}^{-1}$ at $z=+110$ cm). Similarly, a thermal absorption peak in Ge at 139.9 keV [18] allows to set the thermal neutron flux in the irradiation

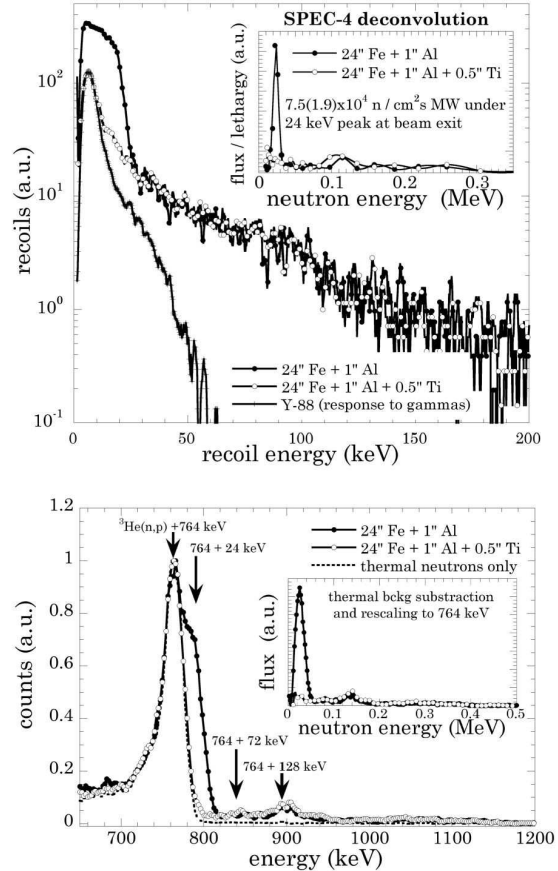


Figure 6. Top: Dramatic effect of a thin Ti post-filter in removing the main 24 keV beam component while allowing contaminations to pass through (see text). Ti filter on and off spectra correspond to the same exposure. Bottom: A lower in resolution (yet similar in features) energy spectrum revealed by a ^3He ionization chamber, used as a rudimentary spectrometer. The normalized response of the detector to a pure thermal neutron field is shown for comparison.

point at $\sim 30 \text{ n cm}^{-2} \text{ s}^{-1} \text{ MW}^{-1}$, a very low value characteristic of Fe filters [7]. The gamma dose at $z=+110$ cm was found to be a very modest 0.3 mRem/hr at full reactor power (240 kW).

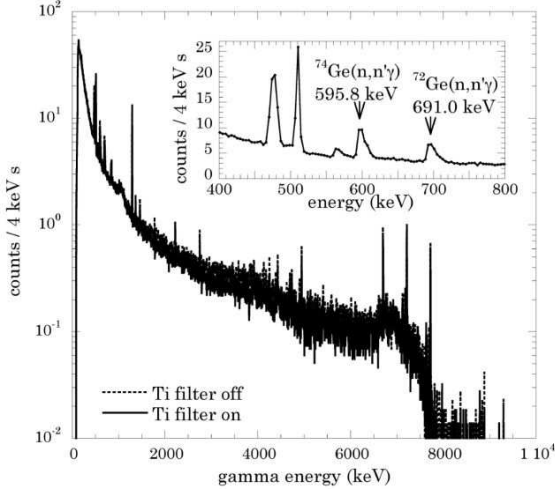


Figure 7. Negligible effect of Ti post-filter on the very small gamma beam contamination, as measured by a HPGe detector. The inset displays characteristic asymmetric peaks from inelastic neutron scattering, used to set limits on beam contamination by fast neutrons (see text). Reactor power was at the present maximum of 240 kW during these measurements.

2.3. Tests of the calibration setup

It is clear from Fig. 2 that a 24 keV neutron beam provides a unique opportunity to produce sub-keV nuclear recoils on any target, much like those expected from reactor antineutrinos. The recoil energy can be selected at will by tagging the neutron scattering angle, θ_n , with a suitable auxiliary neutron detector. The highest possible efficiency in the detection of scattered neutrons is needed if a low power experimental reactor is to be used: Monte Carlo studies of the response of a number of possibilities lead to the choice of a large (5 cm diam. x 7.5 cm long) enriched ${}^6\text{Li}(\text{Eu})$ crystal as optimal for scattered neutrons in the few keV range. While ${}^6\text{Li}$ is typically used for thermal neutron detection, a large crystal of this size allows for efficient moderation of intermediate neutron energies within the crystal itself, followed by capture: at 97% ${}^6\text{Li}$ enrichment, 29% of collimated 24 keV neutrons entering through the front face of this crystal are expected to be

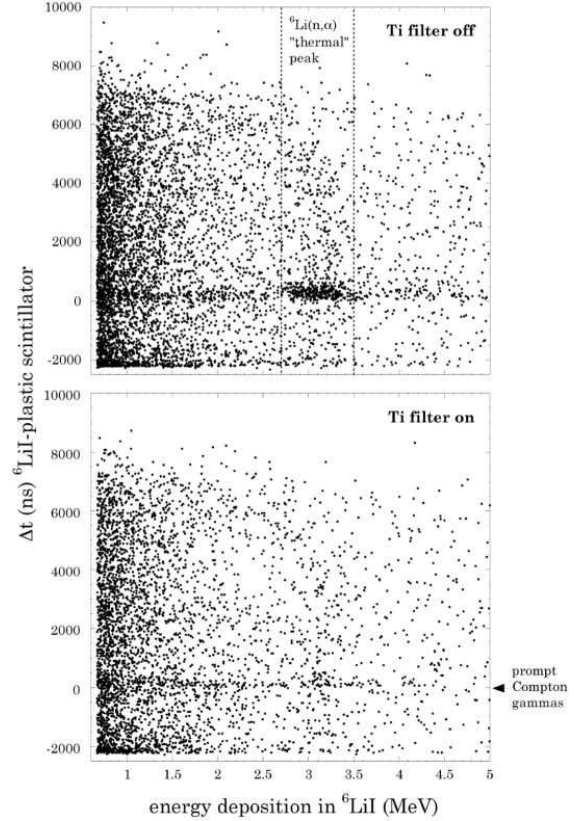


Figure 8. Measured time-difference between low-energy hydrogen recoils in BC-404 plastic scintillator and detection of the scattered neutron via ${}^6\text{Li}(n,\alpha)$. Correlated true-coincidences induced by the 24 keV component of the beam can be seen to vanish in the presence of the Ti post-filter. Both figures correspond to the same exposure.

captured. A second important advantage from this type of detector is the appearance of the ${}^6\text{Li}(n,\alpha)$ absorption “thermal peak” at 3.1 MeV electron equivalent, an energy high enough for most gamma backgrounds to fall below it, allowing for an efficient environmental gamma background reduction. The rate under this “thermal” peak, revealing of the arrival of a scattered neutron, is ~ 100 Hz at full reactor power (240 kW), with just a thin layer of borated silicone as (ther-

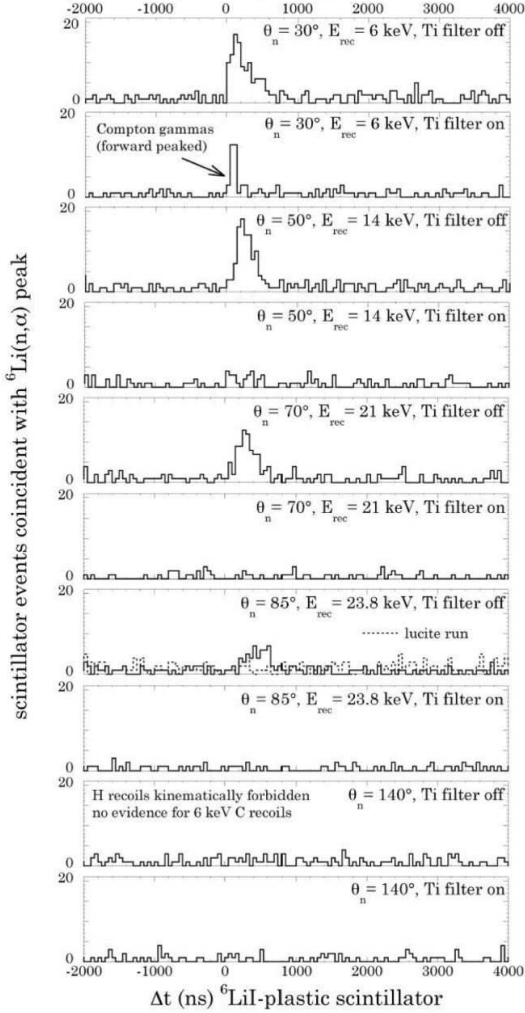


Figure 9. Total of all BC-404 scintillator measurements (see text). An optimal ability to positively identify sub-keV recoils in detectors capable of coherent neutrino detection has been demonstrated in these tests of the UC/KSU beam and setup.

mal neutron) shielding around the crystal. This is a comfortably low figure that ensures an absence of spurious coincidences between the detector under test and the ${}^6\text{Li}(\text{Eu})$ crystal [16].

A repetition of a historic experiment using a

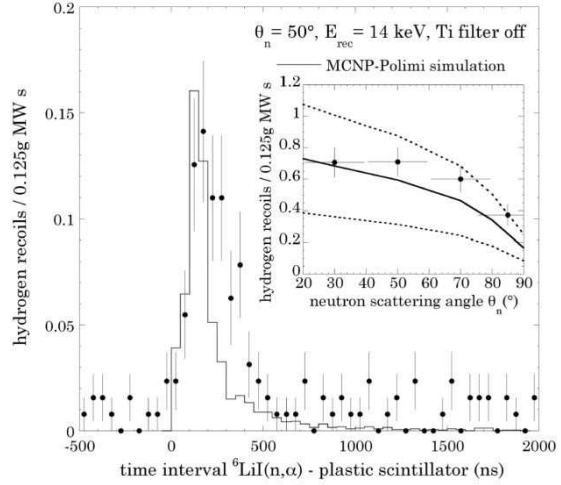


Figure 10. Comparison of time differences between BC-404 hydrogen recoil and ${}^6\text{Li}(\text{Eu})$ neutron capture signals with a MCNP-Polimi [8] simulation devoid of free parameters. The effect of neutron time-of-flight between both detectors and straggling within the ${}^6\text{Li}(\text{Eu})$ scintillator prior to capture is evident. The simulation takes into account the finite timing capabilities of the data acquisition system. Inset: measured rate of true coincidences between hydrogen recoils in BC-404 and the ${}^6\text{Li}(\text{n},\alpha)$ scattered neutron capture signal, as a function of θ_n . The solid line corresponds to Monte Carlo expectations. Dotted lines represent a conservative one sigma uncertainty in these, dominated by a 15% estimated error assigned to each of two Monte Carlo simulations involved.

similar beam was performed to test the full calibration system [17]. In the original work, an unexpectedly-high light yield from sub-keV hydrogen recoils was measured in plastic scintillator, demonstrating the ability to look for slow magnetic monopoles with the MACRO detector [19]. In the present remake, a sample of high yield BC-404 plastic scintillator small enough (0.5 c.c) to ensure avoiding multiple scattering was used as the target detector in front of the beam. Because of the small hydrogen recoil energies involved (24 keV maximum), low light yield of organic scintillators and quenching factors of $O(10)\%$ [17] the signals expected in coincidence with the ${}^6\text{Li}(\text{n},\alpha)$

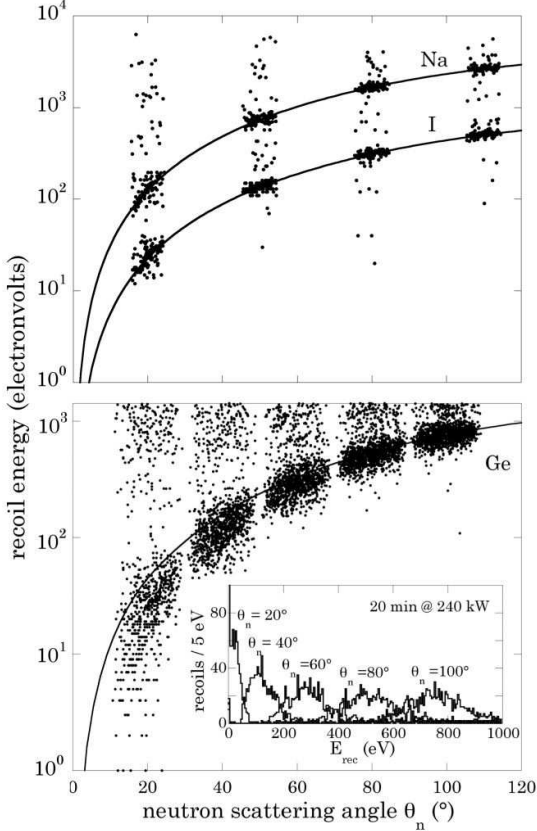


Figure 11. MCNP-Polimi simulated recoil rates and energies in the UC/KSU beam. Solid lines are the kinematic expectations. Top: small (1 c.c.) NaI scintillator. Bottom: 500 g HPGe detector (multiple scattering in this larger crystal leads to a small fraction of events with energy depositions of up to a few keV). The inset shows the signal rates expected in coincidence with the ${}^6\text{LiI}(\text{Eu})$ detector described in the text. This modified-electrode HPGe detector and the results of its calibration in this facility are the subject of a companion paper [4].

peak involve no more than a few photoelectrons, even for a well-matched photomultiplier. Nevertheless a time-coincident excess of events is clearly observed in the absence of the Ti post-filter, to vanish in its presence (Fig. 8). Fig. 9 displays the total of the measurements performed

at different values of θ_n . Several interesting (yet expected) features are present in the data. For instance, the appearance of prompt coincidences due to forward-peaked Compton scattering of gammas only at small θ_n . The neutron time-of-flight between both detectors is also visible (~ 70 ns for 15 cm @ 24 keV), as well as the delay from neutron straggling within the ${}^6\text{LiI}(\text{Eu})$ crystal, in excellent agreement with MCNP-Polimi simulations [8] (Fig. 10). Finally, as expected, no hydrogen recoils were observed at kinematically-forbidden $\theta_n > 90^\circ$. Carbon recoils as low as few keV might nevertheless produce enough scintillation light to be detectable at those angles [20], but the much lower recoil rate expected for these and the short exposure during these first tests (1 hr per angle) did not lead to an observable occurrence. As originally performed in [17], the BC404 scintillator was replaced during a run by an identical sample of lucite to test that coincidences occur from actual recoils in the BC404 and not from Cerenkov light in the photomultiplier glass envelope: no obvious coincidences attributed to the envelope were observed (Fig. 9).

3. CONCLUSIONS

As evidenced by Figs. 8-10, the setup, beam purity and control of backgrounds achieved allows to unequivocally identify events in a detector under test that originate in ultra-low energy nuclear recoils (well below 1 keV for targets heavier than hydrogen), with a convenient ability to select their energy. This is achieved in excellent signal-to-noise conditions, by requesting coincidences with the ${}^6\text{Li}(\text{n},\alpha)$ peak. The additional ability to “switch off” these low-energy recoils by means of the Ti post-filter, while allowing the scarce backgrounds to remain unaffected, provides a convenient and convincing workbench for calibration of coherent neutrino detector technologies. Fig. 11 displays the expected range of recoil energies and signal rates that the beam and calibration setup can provide, for two different target materials.

As discussed in the companion paper [4], at least one detector technology has been developed with all the characteristics needed to attempt an

exciting first reactor measurement of the coherent neutrino scattering cross section. The tools are already in place for the much needed preliminary step, a careful calibration using soft recoils similar to those from reactor antineutrinos.

4. ACKNOWLEDGEMENTS

We are indebted to the instrument design makers at EFI, E. Mendoza, R. Metz, D. Plitt and G. Ward, for the dedication and finesse with which the filter was constructed. Also to A. Cebula, E. Cullens, A. Meyer, L. Retzlaff, C.J. Solomon, Troy Unruh, R. Van Fange, J. Van Meter and the rest of the KSU reactor operators for their generosity and patience in running for many long hours, and their dexterity in keeping reactor poisoning at bay. This work is supported by NSF CAREER award PHY-0239812, NNSA grant DE-FG52-0-5NA25686 and in part by the Kavli Institute for Cosmological Physics through grant NSF PHY-0114422 and a Research Innovation Award No. RI0917 (Research Corporation).

REFERENCES

1. D. Z. Freedman *et al.*, Annu. Rev. Nucl. Sci. **27** (1977) 167.
2. A. Drukier and L. Stodolsky, Phys. Rev. **D30** (1984) 2295.
3. J.I. Collar and Y. Giomataris, Nucl. Instr. Meth. **A471** (2001) 254.
4. P.S. Barbeau, J.I. Collar and O. Tench, “Large-Mass Ultra-Low Noise Germanium Detectors: Performance and Applications in Neutrino and Astroparticle Physics”, submitted to Phys. Rev. C, available from <http://cfcp.uchicago.edu/~collar/co2.pdf>
5. P.S. Barbeau *et al.*, IEEE Trans. Nucl. Sci. **50** (2003) 1285.
6. K. W. Jones and H. W. Kraner, Phys. Rev. **A 11** (1975) 1347.
7. R. C. Block and R. M. Brugger in “Neutron Sources for Basic Physics and Applications”, A. Michandon *et al.* eds., Pergamon, NY, 1983; F.Y. Tsang and R.M. Brugger, Nucl. Instr. Meth. **134** (1976) 441; O. Aizawa *et al.*, J. Nuc. Sci. Tech. **20** (1983) 354; A.V. Murzin *et al.*, Sov. At. Energy **67** (1989) 699; S.V. Musolino *et al.*, Med. Phys. **18** (1991) 806; C.A. Perks *et al.*, Rad. Prot. Dosim. **15** (1986) 31.
8. S.A. Pozzi *et al.*, Nucl. Instr. Meth. **A513**, 550 (2003).
9. *MCNP, A General Monte Carlo N-Particle Transport Code*, J.F. Briesmeister ed., Los Alamos National Laboratory, LA-12625-M, 1993.
10. 3N5 pure iron (ESPI, Ashland, Oregon 97520, USA).
11. Model 27044 (LND, Oceanside, New York 11572, USA).
12. Proteus Inc., Chagrin Falls, Ohio 44022, USA.
13. Alloy 1100, commercially pure (99%) aluminum.
14. W.H. Miller, Nucl. Instr. Meth. **A279** (1989) 546.
15. Oak Ridge National Laboratory, RSICC peripheral shielding routine collection, *SPEC-4, Calculated Recoil Proton Energy Distributions from Monoenergetic and Continuous Spectrum Neutrons*.
16. The original ${}^6\text{LiI}$ crystal used for these measurements had been salvaged and reencapsulated from a larger, partially-hydrated and fractured unit, exhibiting a degraded resolution. A brand new crystal, 5 cm in diameter and 1.5 cm long has been developed by Proteus Inc. At the expense of a loss in 24 keV neutron efficiency by a factor ~ 3 , the background rate under the thermal peak is reduced by a factor ~ 20 in this unit, greatly improving the capabilities of the setup.
17. D.J. Ficenc *et al.*, Phys. Rev. **D36** (1987) 311; S.P. Ahlen *et al.*, Phys. Rev. Lett. **55** (1985) 181.
18. R. Wordel *et al.*, Nucl. Instr. Meth. **A369** (1996) 557.
19. M. Ambrosio *et al.*, Eur. Phys. J. **C25** (2002) 511.
20. J. Hong *et al.*, Astropart. Phys. **16** (2002) 333.